

Swarthmore College

Works

Engineering Faculty Works

Engineering

7-1-2016

Diagnostic Ultrasound High Mechanical Index Impulses Restore Microvascular Flow In Peripheral Arterial Thromboembolism

T. R. Porter

S. Radio

J. Lof

E. Carr Everbach

Swarthmore College, ceverba1@swarthmore.edu

J. E. Powers

See next page for additional authors

Follow this and additional works at: <https://works.swarthmore.edu/fac-engineering>



Part of the [Engineering Commons](#)

[Let us know how access to these works benefits you](#)

Recommended Citation

T. R. Porter, S. Radio, J. Lof, E. Carr Everbach, J. E. Powers, J. E. Powers, F. Vignon, W. T. Shi, and F. Xie. (2016). "Diagnostic Ultrasound High Mechanical Index Impulses Restore Microvascular Flow In Peripheral Arterial Thromboembolism". *Ultrasound In Medicine And Biology*. Volume 42, Issue 7. 1531-1540. DOI: 10.1016/j.ultrasmedbio.2016.02.001
<https://works.swarthmore.edu/fac-engineering/95>

This work is brought to you for free by Swarthmore College Libraries' Works. It has been accepted for inclusion in Engineering Faculty Works by an authorized administrator of Works. For more information, please contact myworks@swarthmore.edu.

Authors

T. R. Porter, S. Radio, J. Lof, E. Carr Everbach, J. E. Powers, J. E. Powers, F. Vignon, W. T. Shi, and F. Xie



Published in final edited form as:

Ultrasound Med Biol. 2016 July ; 42(7): 1531–1540. doi:10.1016/j.ultrasmedbio.2016.02.001.

Diagnostic Ultrasound High Mechanical Index Impulses Restore Microvascular Flow in Peripheral Arterial Thromboembolism

Thomas R. Porter, MD¹, Stanley Radio, MD¹, John Lof, MS¹, Carr Everbach, PhD², Jeffrey E. Powers, PhD³, Francois Vignon, PhD⁴, William T. Shi, PhD⁴, and Feng Xie, MD¹

¹University of Nebraska Medical Center, Omaha, Nebraska

²Swarthmore College, Swarthmore, PA

³Philips Healthcare, Bothell, Washington

⁴Philips Research North America, Briarcliff Manor, New York

Abstract

We sought to explore mechanistically how intermittent high mechanical index (MI) diagnostic ultrasound impulses restore microvascular flow. Thrombotic microvascular obstruction was created in the rat hindlimb muscle of 36 rats. A diagnostic transducer confirmed occlusion with low MI imaging during an intravenous microbubble infusion. This same transducer was used to intermittently apply an MI that produced stable or inertial (IC) cavitation for 10 minutes through a tissue mimicking phantom. A nitric oxide (NO) inhibitor L-NAME was pre-administered in six rats. Plateau microvascular contrast intensity quantified skeletal microvascular blood volume (MBV), and post mortem staining examined for perivascular hemorrhage. Intermittent IC impulses produced the greatest recovery of MBV ($p < 0.0001$; ANOVA). NO inhibition did not affect the skeletal MBV improvement, but did result in more perivascular hemorrhage. IC inducing pulses from a diagnostic transducer can reverse microvascular obstruction following acute arterial thromboembolism. NO may prevent unwanted bioeffects from these IC pulses.

Keywords

Microvascular obstruction; diagnostic ultrasound; cavitation; nitric oxide

Corresponding Author: Thomas R. Porter, M.D., University of Nebraska Medical Center, Omaha, NE 68128, trporter@unmc.edu, Phone: 402-559-8150.

Conflicts of Interest

Doctor Porter has research equipment support from Philips Healthcare and grant support from Lantheus and Astellas Pharma. He is on the speaker's bureau for Bracco Diagnostics.

Publisher's Disclaimer: This is a PDF file of an unedited manuscript that has been accepted for publication. As a service to our customers we are providing this early version of the manuscript. The manuscript will undergo copyediting, typesetting, and review of the resulting proof before it is published in its final citable form. Please note that during the production process errors may be discovered which could affect the content, and all legal disclaimers that apply to the journal pertain.

INTRODUCTION

Microvascular obstruction (MVO) downstream from acute arterial thrombosis remains a critical factor preventing clinical recovery following acute myocardial infarction and stroke (Bekkers et al. 2010; Wu 2012; Nour et al. 2013). Thrombotic microembolization plays a critical role in MVO, as fibrin and activated platelets with the microemboli interact with microvascular endothelium to initiate several inflammatory processes that propagate and sustain MVO (Stokes and Granger 2012). Ultrasound induced cavitation of microbubbles at prolonged pulse durations and high mechanical indices has been proposed as a method of dissolving microvascular thrombi (Stokes and Granger 2012). Initial in vivo studies in microvascular preparations have demonstrated microvascular thrombus dissolution with intra-arterial administration of microbubbles combined with long pulse duration low frequency ultrasound (Leeman et al. 2012). Although these studies were also done in the presence of minimal beam attenuation, high mechanical index (1.0-2.0) impulses from a diagnostic transthoracic transducer, during a systemic intravenous microbubble infusion, have also appeared to improve microvascular flow in acute myocardial infarction, where significant beam attenuation was present (Pacella et al. 2015; Xie et al. 2009; Xie et al. 2011). Since improvement in microvascular flow in these studies was seen even without epicardial recanalization, it is possible that ultrasound induced cavitation of microbubbles may improve flow via other mechanisms, such as stimulation of nitric oxide (NO) release (Xie, et al. 2013; Siegel et al. 2004). The purpose of this paper was to utilize an established model of microvascular embolization in a rat hindlimb skeletal muscle preparation (Leeman et al. 2012) to determine whether modified high mechanical index (MI) impulses from a diagnostic transducer could restore skeletal blood perfusion when varying degrees of attenuation are present. Secondly, we sought to determine what role NO production plays in mediating any improvements in microvascular flow induced by diagnostic ultrasound.

MATERIALS AND METHODS

Detection of Inertial and Stable Cavitation Induction with a Diagnostic Transthoracic Ultrasound System

The Institutional Animal Care and Use Committee of the University of Nebraska Medical Center approved this entire study (IACUC #13-096-02-FC). All animal experiments conformed to the NIH guidelines (Guide for the Care and Use of Laboratory Animals: Eighth Edition, National Research Council, 2010). Throughout the study, a software-modified commercial ultrasound scanner iE33 with a sector imaging probe S5-1 (Philips Healthcare, Andover, MA) was employed for microbubble cavitation imaging. Cavitation imaging is based on the spectral analysis of acoustic signals radiated by the cavitating microbubbles: ultraharmonics of the excitation frequency indicate stable cavitation (SC), whereas noise bands indicate inertial cavitation (IC). Long (20 and 44 μ s) 1.6 MHz “diagnostic ultrasound pulses” were transmitted to excite microbubbles within the region of interest and backscattered radiofrequency (RF) beam-formed signals were acquired with an internal RF data acquisition board and initially saved in the scanner’s hard drive. The RF data were then transferred to an external PC and processed offline for cavitation signatures

within the region of interest. More details of the cavitation imaging system are given in our previous paper (*Vignon et.al. 2013*).

Initial studies were performed in four Sprague Dawley male rats (weights 350-600 grams, Charles River Laboratories, Wilmington, Massachusetts) to confirm what mechanical index (MI) settings on the diagnostic transducer were producing inertial and stable cavitation, and validate the ability of the imaging and therapeutics system to detect IC. All rats were anesthetized with isoflurane (Isothesia, Abbott Laboratories, North Chicago, Illinois) (1-3%). The right external jugular vein was cannulated with a 22 G angio-catheter (BD Insyte Autoguard Winged, Becton Dickinson Infusion Therapy Systems, Inc., Sandy, Utah) for microbubble infusions. Rat body temperature was maintained with a heating pad (Maxitherm vinyl blanket, Med Vet International Mettawa, Illinois). At the end of the procedure the rats were euthanized by bilateral thoracotomy while still under general anesthesia.

The rats underwent degloving of the left hind limb and subsequently were placed in the right lateral position. This muscle microvascular preparation contains microvessels ranging from capillaries to small (25-50 micron), medium (50-100 micron), and large arterioles (100-200 microns in diameter). (Leeman et al. 2012) The ultrasound probe S5-1 was positioned just anterior to the left hind limb to horizontally scan the long axis plane of the left hind limb muscle. A 10% Definity (Lantheus Medical Imaging, Inc. North Billerica, Massachusetts) microbubble infusion (120 uL/min) was initiated in the external jugular vein during which imaging was performed with the transducer using a low MI (0.1) amplitude modulation mode for microbubble contrast detection within the microvasculature. This microbubble infusion rate produced consistent microvascular enhancement without shadowing at the 0.1 MI setting. Microbubble response signatures were analyzed by examining the radiofrequency (RF) signals returning to the transducer and comparing it to those from passive cavitation detectors (PCD's) as described below. The diagnostic ultrasound pulses were applied through custom urethane tissue mimicking phantoms (TMP) (Computerized Imaging Reference Systems, Inc. (CIRS), Norfolk, Virginia) that created either three or six centimeter standoffs between the preparation and the transducer (Figure 1). The attenuation induced by the TMPs was calculated according to their thickness and manufacturer's specified attenuation coefficients, which for this TMP was 0.49 db/cm²/MHz. When a stable microbubble presence was visualized with low MI imaging, backscattered radiofrequency (RF) contrast signal traces at increasing MIs were recorded by the scanner's RF data acquisition board, and the signals processed to confirm that the specific outputs produced either non-destructive stable cavitation (NSC), destructive stable cavitation (SC), or inertial cavitation (IC) based on characteristic features of the averaged spectra of the signals over the region of interest corresponding to the skeletal muscle preparation. A narrow (0.4 MHz) frequency band of 2.2 to 2.6 MHz for the bandpass filter was used to detect stable cavitation. Modification for the bands of choice was not needed from animal to animal because the passband width was largely dependent on the contrast bubble resonant response in the imaging frequency band as well as the spectral resolution determined by the transmit pulse length.

The 20 MHz PCD's (Model IX-116, UTX, Inc. Holmes, New York) were confocally placed in the buffer *below* the TMPs to monitor for inertial cavitation. Correlations with intensity of IC detection from the 20 MHz PCDs and binary IC detection by the RF data acquisition board were performed. These correlations were examined using a 20 μ s therapeutic impulse duration from the diagnostic transducer, and not for shorter pulsing durations used for imaging because spectral resolution of the detection method was too low for these pulse durations. The 20 MHz PCDs have a 1 MHz bandwidth at this frequency, or 5%; i.e.; filters extend from approximately 19.5 to 20.5 MHz with rapid drop off (24 dB/octave) at the edges of the passband. Their focal region is defined by the width of the sensitive region, which have -3 dB focal widths of 1 mm in diameter and about 5 mm long (along the focal axis). 20 MHz frequencies produced or scattered within this volume that result in spherically spreading waves will be picked up by the detector, and thus direct acoustic emissions within this volume will be picked up as well as scattering from any structures.

Subsequent Microvascular Embolization Studies

A total of 36 rats (six groups of six animals) were then tested. Two groups received intermittent IC inducing impulses in the presence of either a three or six centimeter thick TMP, two groups received intermittent SC inducing impulses in the presence of either a three or six centimeter TMP, and one group received just low MI (0.1 MI) imaging alone through a three centimeter TMP. This has been shown to induce non-destructive stable cavitation or NSC (Vignon 2013). A sixth group received intermittent IC inducing impulses through a three centimeter TMP after the rats had received a 30 mg/kg dose of the nitric oxide inhibitor L-N ω -Nitroarginine methyl ester (L-NAME, Sigma-Aldrich Chemie GmbH, Buchs, Switzerland) (Fitch RM 2007).

Rats were placed on a custom designed stage and polyethylene tubing (BD IntramedicTM PE 10, Becton, Dickinson and Co., Franklin Lakes, New Jersey) advanced from the right femoral artery to the aorto-iliac bifurcation to deliver emboli directly to the left hind limb microcirculation. The S5-1 transducer was fitted with either the 3 or 6 centimeter thick TMP and then clamped into a fixed constant position such that the imaging beam was placed along the long axis of the muscle preparation. At this point, a 20% Definity infusion (170 μ liter/minute; 2.0×10^8 microbubbles/minute) was initiated and baseline low MI (0.1) non destructive imaging utilized to examine microvascular contrast enhancement This slightly higher infusion rate was chosen because of the slower blood flow expected following thrombo-embolization. The Definity infusion continued until completion of all treatments and skeletal MBV assessments.. Heart rate and oxygen saturation (Mouse Ox system; STARR Life Sciences Corporation, Oakmont, Pennsylvania) were monitored during all infusions and treatments.

Although brief high MI impulses are utilized diagnostically for replenishment kinetics and microvascular blood flow estimations, they were not performed in this study because of a potential treatment effect that may also occur from the high MI.

Porcine venous blood was obtained, allowed to form thrombi, and then passed through a series of increasing smaller bore needles (18 to 30G, Becton, Dickinson and Co., Franklin Lakes, New Jersey) and finally a 200 micron micropore filter (CellMicroSieves, BioDesign

Inc., Carmel, New York) to create microthrombi (all sized < 200 microns). Serial 300 uliter injections were given until a visually evident reduction in skeletal muscle contrast intensity (reflecting MBV) throughout the visualized portion of the preparation was obtained for 10 minutes during low MI imaging. If a return of contrast signal occurred during this time period, a repeat 300 uliter injection was given and the 10 minute time period repeated.

Randomization to treatment assignment was based on an internet based system (Randomness and Integrity Services Ltd. Dublin, Ireland) to one of the six treatment groups. Each treatment (other than low MI non destructive imaging alone) was applied in an intermittent fashion (five seconds IC or SC inducing pulse, five seconds off) to allow for microbubble replenishment in between the therapeutic impulses. This five second “off time” was what appeared to produce complete contrast replenishment in the initial normal rat studies.. Total treatment times were for 10 minutes, at which point reassessments of skeletal MBV were made once a stable plateau intensity was visually achieved.

The plateau skeletal muscle intensity was used to estimate skeletal MBV (Leeman et al. 2012). Skeletal MBV measurements were measured by an experienced reviewer (FX) who had no knowledge of treatment assignment. A 17×5 mm rectangular region of interest was placed in a fixed central location in the muscle preparation during low MI imaging. Intensity measurements were determined with QLAB software (Version 9.0, Royal Philips, Amsterdam, The Netherlands). The averaged digital intensity was then obtained under baseline conditions, after persistent occlusion, and after completion of a 10 minute randomized treatment.

Post mortem Sectioning of Muscle Preparations

Once post treatment assessments of skeletal MBV were digitally acquired, the rats were sacrificed and the skeletal muscle section that corresponded to the imaging plane was sectioned and placed in formalin. 4 micron sections of the mid and lateral portions of the imaged muscle preparation were obtained for analysis of thrombus and perivascular hemorrhage by hematoxylin and eosin staining (Menci 2013). Each section contains 30-40 small vessel, 10-12 medium sized, and 2-5 large vessels. Using this staining method, only residual thrombi evident in small (25-50 micron) and medium to large sized (50-100 micron size) microvessels could be identified and not capillary thrombi. Any residual thrombus creating >50% obstruction in any arteriole was considered significant. Vessels were also examined for evidence of perivascular hemorrhage, which was graded as absent or mild (1 or less foci of hemorrhage in a $10\times$ scanning magnification), versus moderate (> 1 foci). The entire analysis (for residual significant thrombus or perivascular hemorrhage) was performed by an independent experienced cytopathologist (SJR) blinded to treatment assignment. Intra-observer agreement on grading of perivascular hemorrhage severity and presence or absence of residual thrombus were performed by randomly repeating 20 slides from 10 rat samples on a separate date.

Statistical Analysis

Comparisons of skeletal MBV changes within groups were determined with paired testing. Changes in SMBV between groups were compared with a multiple comparisons procedure

(ANOVA). Comparisons of the presence or absence of residual small artery or vein thrombi between groups, or presence of significant perivascular hemorrhage, were determined with contingency tables (Fisher Exact Test). The Fisher Exact test was performed because the proportions were less than five in certain outcomes (Lametz K 1978). A p value of <0.05 was considered significant in all comparisons.

RESULTS

Table 1 demonstrates the focal depth and calculated peak negative pressures for the 0.8 and 1.6 MI settings. Table 2 demonstrates the averaged root mean square (RMS) values from the 20 MHz PCDs near the hind limb microvasculature in the multiple measurements from the four rats, and how this correlated with the SC and IC inducing impulses based on RF signals analyzed by the transducer and iE33 system. RF analysis of signals returning to the transducer indicated minimal ultraharmonics and low broadband noise at MI's of 0.3 or less, indicating non destructive stable cavitation (NSC). Dominant ultraharmonics were visible at an MI = 0.8 indicating strong SC. Elevated broadband noise without salient ultraharmonics were present at MI = 1.6 indicating dominant IC. There was a significant increase in the RMS values from the PCDs (indicative of strong inertial cavitation from collapsing microbubbles) for IC inducing impulses, which dropped off significantly with SC inducing impulses at the 0.8 MI setting from the diagnostic system. At MI's of 0.3, virtually no collapsing microbubbles were detected by the PCD's. Therefore, for subsequent studies, NSC was <0.3 MI, SC was 0.8 MI, and IC was 1.6 MI. All pulse durations were 20 μ s.

Comparison of IC with SC and NSC in Restoring Microvascular Flow

Injection of the microvascular thrombi consistently created a reduction in plateau contrast intensity within the skeletal muscle (Figure 2). The intermittently applied IC inducing impulses (both with the 3 and 6 cm TMP) produced a significant increase in skeletal MBV (Figure 3), while the intermittent SC inducing impulses produced a smaller, but significant, increase in MBV only in the presence of the 3 cm thick TMP. NSC alone did not produce an increase in MBV. No changes in oxygen saturation or heart rate were noted in any animal during any of the randomized treatments.

L-NAME was only tested with the setting that produced an optimal increase in skeletal MBV (which were IC inducing impulses with a 3 centimeter thick TMP). Prior treatment L-NAME did not have an effect on the change in skeletal MBV changes with IC inducing impulses (Figures 2 and 4).

Post mortem Staining

Up to 3 sections were analyzed in each rat for residual arteriolar thrombi and evidence perivascular or interstitial hemorrhage (Table 2). Residual $>50\%$ thrombi within small or medium sized vessels (Figure 5) were seen with lowest frequency in the L-NAME treated rats who had IC inducing pulses intermittently applied through a 3 cm TMP ($p<0.05$ compared to both SC inducing pulse applied through 3 and 6 cm TMP and IC inducing pulses through a 3 cm thick TMP in the absence of L-NAME). Also, moderate degrees of perivascular hemorrhage (Figure 6 example) were seen with highest frequency in the L-

NAME pre-treated group ($p < 0.01$ compared to SC inducing impulses). Intra-observer agreement was 100% ($n = 20$ slides) for presence of residual thrombus, and 95% for grading of peri-vascular hemorrhage score.

Conclusions

Intermittently applied high mechanical index impulses from a modified diagnostic transthoracic transducer can restore microvascular blood volume following thrombotic microembolization, even in the presence of significant attenuation. This beneficial effect is not affected by NO inhibition, but NO may play an important role in reducing unwanted bioeffects from the impulses.

DISCUSSION

This study for the first time demonstrates the potential for IC inducing pulses from a modified diagnostic transducer to restore MBV following embolic occlusion. The blood volume was restored even in the presence of six centimeters of tissue mimicking material, indicating the potential for diagnostic ultrasound high MI impulses to resolve microvascular thrombosis in settings of significant attenuation such as in transthoracic or trans-temporal bone applications. Transthoracic and transcranial windows vary extensively from patient to patient, and thus we specifically assessed what effect two different degrees of attenuation would have on the ability of these guided high mechanical index impulses to restore microvascular flow. There is a practical limitation here, in that all commercially available systems, like the one in this study, have limits on what MI can be used. This, in turn, would be a limit on how much the amplitude could be increased. We discovered that MI's within FDA limits (0.8 and 1.6) are effective, with the 1.6 MI being effective at both three and six centimeter tissue mimicking standoffs. Although IC inducing impulses appear more effective, the role of NO in mediating bioeffects has not been further elucidated until the current study. On the one hand, NO inhibition appeared to result in more cavitation induced perivascular hemorrhage. On the other hand, post mortem staining also demonstrated greater clearance of thrombus from small and medium sized microvessels with NO inhibition. Since these vessels make up only a small portion of the overall microvascular volume, we did not see an overall change in MBV recovery by contrast low MI imaging with IC inducing impulses in the presence of NO inhibition.

Several in vitro observations have demonstrated the potential for both SC and IC to augment fibrinolysis (Bader et.al. 2015, Datta et al. 2006; Everbach et al. 2000; Hitchcock et.al. 2011, Kodama et al.1999; Prokop et al. 2007; Suchkova et al.2002). IC inducing pulses have the potential for creating liquid jets that may be responsible for the penetration of thrombus recently observed in vitro with high speed cameras (Chen et al. 2014). Liquid jet penetration from collapsing microbubbles may explain why greater thrombus dissolution occurs with IC than SC inducing pulses. This same bioeffect, however, could also explain why significant perivascular hemorrhage may also occur due endothelial cell penetration. High MI ultrasound, in relatively un-attenuated settings, may cause hemorrhage and even cell death in the presence of microbubbles (Ay et al. 2001; Miller et al. 2006) and is a potential limitation of this otherwise non-invasive method to treat microvascular obstruction. It is interesting to

note, though, that the perivascular hemorrhage was not observed with the IC inducing pulses in the absence of L-NAME, indicating NO may have played a role in prevention of perivascular hemorrhage. Ultrasound has been shown to increase flow downstream from an obstructed epicardial or peripheral blood vessel via an NO-dependent mechanism (Siegel et al 2004; Xie et al 2013). This IC-induced increase in flow in the microvasculature has recently been shown to be primarily due to increases in red blood cell flux velocity (Belcik et al. 2015). Since the high MI impulses that increased red blood cell velocity were similar to the MI's used to induce IC in our study, it is possible that the higher flux velocity resulted in less exposure of the liquid jets created by cavitating microbubbles to the vessel wall, and may explain why significant perivascular hemorrhage was seen only following NO inhibition.

The higher red blood cell flux induced by NO production from IC of microbubbles may have also played a role in why we observed more residual thrombi in small and medium sized arterioles following NO inhibition, as the higher flux velocity may also reduce cavitating microbubble exposure to thrombi in these vessels. However, it appears these arterioles appeared to contribute minimally to the overall tissue blood volume and thus had no effect on overall microvascular recovery. Overall, it appears that IC inducing impulses from a diagnostic transducer result in both mechanical microvascular thrombus disruption and NO release. NO may play a critical role in preventing unwanted bioeffects in addition to its known effect in this setting of preventing platelet recruitment (Loscalzo. 2001).

Although IC inducing pulses were most effective in restoring microvascular blood volume, SC inducing pulses were also effective but only when using a three centimeter TMP. The process of SC can still elicit clot erosion from a strong shear force near the oscillating bubble surface when a bubble is close to the clot surface, or from destruction due to the oscillating bubble inside the clot. The thicker 6 cm TMP not only would decrease the strength of the stable oscillation, but also alter the ultrasound focusing capabilities. The S5-1 transducer in this study can produce a strong focus only at small depths of 3 to 5 cm. This lack of focusing capability may explain why other in vitro investigations have not observed thrombus dissolution without tPA when eliciting SC from a 120 kilohertz transducer, even in the absence of tissue mimicking attenuation (Bader et.al. 2015).

Study Limitations

The optimal generation of SC inducing pulses has been shown to be at longer pulse durations than the ones used in this study (Hitchcock 2011). In other studies, though, the PCD was a separate transducer placed at right angles to the therapy transducer, and thus there was no limit to the length of transmitted pulse. In addition, the cavitation detection zone was fixed as the small region where the ultrasound beams crossed each other. In our setup, an imaging scanner was employed for both therapy and cavitation detection,, so the pulse length was limited. A relative shorter pulse of 20 μ s was used for a better resolution (in depth) of the cavitation detection although a longer pulse would result in a greater SC (ultraharmonic) signal strength. Very low frame rates (equivalent to PRF for the PCD) were used to allow adequate replenishment of contrast microbubbles between frames. The transmitted pulses amplitude was increased for sufficient (but not optimal) ultraharmonic

strength. However, there are certain advantages of the imager based cavitation detection system, in that you have near simultaneous image guidance, and the detection zone is spatially adjustable (not fixed), and thus is feasible for use in animal or human studies.

In this study, we tested only the 20 μ s pulse duration at different mechanical indices and degrees of tissue attenuation. It is unclear if similar findings would be seen at the short diagnostic ultrasound imaging pulse durations of 5 μ s or less. We also only tested the effect of NO inhibition with only one ultrasound setting, but it was the one that produced the highest degree of skeletal MBV recovery.

The vasodilatory effects of NO release have been observed with both intermediate and high mechanical index pulses from a diagnostic transducer (Belcik 2015), and thus its beneficial effect would be expected at both the SC and IC setting used in this study. We only tested the effects of NO suppression in the setting most likely to induce unwanted bioeffects (inertial cavitation inducing pulses with the least degree of attenuation of the ultrasound beam). Clinically, one would not consider doing ultrasound induced thrombus dissolution in the presence of a nitric oxide synthase inhibitor, since any added beneficial effect of increased recanalization would be offset by increased capillary hemorrhage and vasoconstriction. Nonetheless, we cannot determine whether unwanted bioeffects would have occurred with NO inhibition at the other settings. We did not determine what effect diagnostic ultrasound induced IC or SC had on skeletal microvascular flow, since we did not want to utilize the high MI impulses used diagnostically to measure red blood cell velocity in the control groups because of their potential therapeutic effect. Furthermore, the infusion rate (140 μ l/min of a 20% Definity dilution) required to achieve optimal skeletal muscle contrast enhancement was higher than that required (per volume) in humans for cardiac imaging. Finally, Table 1 demonstrates that there is substantial loss of peak negative pressure as the degree of tissue between the transducer and microvasculature is increased, which may affect both the presence and magnitude of inertial cavitation induced. This attenuation may reduce the potential for effective thrombolysis in larger sized patients, or in patients with greater degrees of attenuation of the beam.

Acknowledgements

The authors want to acknowledge Carol Gould for her assistance with the preparation of this manuscript.

Funding Source:

This study was supported by National Institutional Health Grant No. NIH R21 EB015163

REFERENCES

- Ay T, Havaux X, Van Camp G, Campanelli B, Gisellu G, Pasquet A, Deneff JF, Melin JA, Vanoverschelde JL. Destruction of contrast microbubbles by ultrasound: effects on myocardial function, coronary perfusion pressure, and microvascular integrity. *Circulation*. 2001; 104:461–466. [PubMed: 11468210]
- Bekkers SCAM, Yazdani SK, Virmani R, Waltenberger J. Microvascular Obstruction. Underlying Pathophysiology and Clinical Diagnosis. *J. Am. Coll. Cardiol*. 2010:1649–1660. [PubMed: 20394867]

- Belcik JT, Mott BH, Xie A, Zhao Y, Kim S, Lindner NJ, Ammi A, Linden JM, Lindner JR. Augmentation of limb perfusion and reversal of tissue ischemia produces by ultrasound-mediated microbubble cavitation. *Circ Cardiovasc. Imaging*. 2015; 8:ii, e002979.
- Chen X, Leeman JE, Wang J, Pacella JJ, Villanueva FS. New insights into mechanisms of sonothrombolysis using ultra-high-speed imaging. *Ultrasound Med Biol*. 2014; 40:258–262. [PubMed: 24139920]
- Datta S, Coussios CC, McAdory LE, Tan J, Porter T, De Courten-Myers G, Holland CK. Correlation of cavitation with ultrasound enhancement of thrombolysis. *Ultrasound Med Biol*. 2006; 32:1257–1267. [PubMed: 16875959]
- Everbach EC, Francis CW. Cavitation mechanisms in ultrasound-accelerated thrombolysis at 1 MHz. *Ultrasound Med Biol*. 2000; 26:1153–1160. [PubMed: 11053750]
- Fitch RM, Vergona R, Sullivan ME, Wang YX. Nitric oxide synthase inhibition increases aortic stiffness measured by pulse wave velocity in rats. *Cardiovasc Res*. Aug 1.2001 51:351–8. [PubMed: 11470475]
- Kodama T, Tatsuno M, Sugimoto S, Uenohara H, Yoshimoto T, Takayama K. Liquid jets, accelerated thrombolysis: A study for revascularization of cerebral embolism. *Ultrasound Med Biol*. 1999; 25:977–983. [PubMed: 10461727]
- Larntz K. Small-sample comparisons of exact levels for chi-squared goodness-of-fit statistics. *Journal of the American Statistical Association*. 1978; 73:253–263. (1978).
- Leeman JE, Kim JS, Yu FTH, Chen X, Kim K, Wang J, Chen X, Villanueva FS, Pacella JJ. Effect of Acoustic Conditions on Microbubble-Mediated Microvascular Sonothrombolysis. *Ultrasound Med Biol*. 2012; 38:1589–1598. [PubMed: 22766112]
- Loscalzo J. Nitric oxide insufficiency, platelet activation, and arterial thrombosis. *Circ Res*. 2001; 88:756–762. [PubMed: 11325866]
- Menci S, Garz C, Solveig N, Braun H, Gob E, Homola G, Heinze H-J, Reymann KG, Kleinschnitz C, Schrei S. Early microvascular dysfunction in cerebral small vessel disease is not detectable on 3.0 Tesla magnetic resonance imaging: a longitudinal study in spontaneously hypertensive stroke-prone rats. *Experimental Translational Stroke Med*. 2013; 5:8.
- Miller DL, Driscoll EM, Dou C, Armstrong WF, Lucchesi BR. Microvascular permeabilization and cardiomyocyte injury provoked by myocardial contrast echocardiography in a canine model. *J Am Coll Cardiol*. 2006; 47:1464–1468. [PubMed: 16580537]
- Nour M, Scalzo F, Liebeskind DS. Ischemia-reperfusion injury in stroke. *Interv. Neurol*. 2013; 1:185–99. [PubMed: 25187778]
- Pacella JJ, Brands J, Schnatz FG, Black JJ, Chen X, Villanueva FS. Treatment of microvascular micro-embolization using microbubbles and long-tone-burst ultrasound: an in vivo study. *Ultrasound Med Biol*. 2015; 41:456–64. [PubMed: 25542487]
- Prokop AF, Soltani A, Roy RA. Cavitation Mechanisms in Ultrasound-Accelerated Fibrinolysis. *Ultrasound Med Biol*. 2007; 33:924–933. [PubMed: 17434661]
- Siegel RJ, Suchkova VN, Miyamoto T, Luo H, Baggs RB, Neuman Y, Horzewski M, Suorsa V, Kobal S, Thompson T, Echt D, Francis CW. Ultrasound energy improves myocardial perfusion in the presence of coronary occlusion. *J Am Coll Cardiol*. 2004; 44:1454–1458. [PubMed: 15464327]
- Stokes KY, Granger DN. Platelets: a critical link between inflammation and microvascular dysfunction. *J Physiol*. 2012; 590:1023–34. [PubMed: 22183721]
- Suchkova VN, Baggs RB, Sahni SK, Francis CW. Ultrasound improves tissue perfusion in ischemic tissue through a nitric oxide dependent mechanism. *Thromb Haemost*. 2002; 88:865–70. [PubMed: 12428107]
- Vignon F, Shi WT, Powers JE, Everbach EC, Liu J, Gao S, Xie F, Porter TR. Microbubble cavitation imaging. *IEEE Trans Ultrason Ferroelectr Freq Control*. 2013; 60:661–70. [PubMed: 23549527]
- Wu KC. CMR of microvascular obstruction and hemorrhage in myocardial infarction. *J. Cardiovasc. Magn. Reson*. 2012; 14:68. [PubMed: 23021401]
- Xie F, Lof J, Matsunaga T, Zutshi R, Porter TR. Diagnostic ultrasound combined with glycoprotein IIb/IIIa-targeted microbubbles improves microvascular recovery after acute coronary thrombotic occlusions. *Circulation*. 2009; 119:1378–1385. [PubMed: 19255341]

- Xie F, Slikkerveer J, Gao S, Lof J, Kamp O, Unger E, Radio S, Matsunaga T, Porter TR. Coronary and microvascular thrombolysis with guided diagnostic ultrasound and microbubbles in acute ST segment elevation myocardial infarction. *J Am Soc Echocardiogr.* 2011; 24:1400–1408. [PubMed: 22037348]
- Xie F, Gao S, Wu K, Lof J, Radio S, Vignon F, Shi W, Powers J, Unger E, Everbach EC, Liu J, Porter TR. Diagnostic Ultrasound Induced Inertial Cavitation to Non-Invasively Restore Coronary and Microvascular Flow in Acute Myocardial Infarction. *PloS One.* 2013; 8:e69780. [PubMed: 23922797]

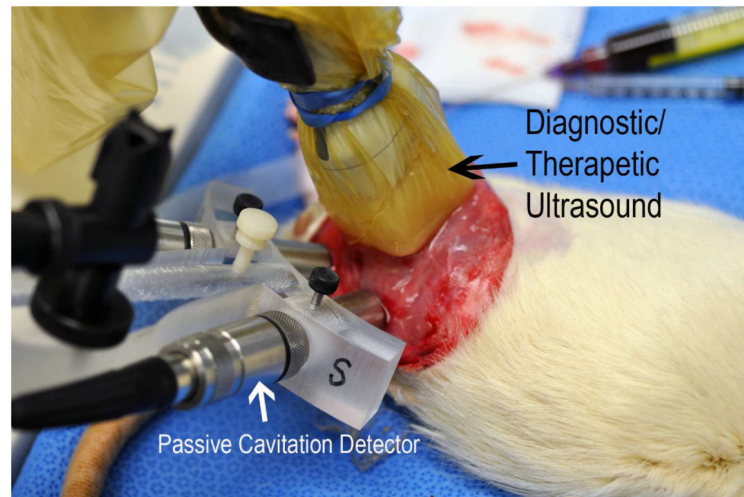


Figure 1. Location of the diagnostic ultrasound transducers applying IC and SC impulses through a tissue mimicking phantom, and the passive cavitation detectors which verified the presence and intensity (in root mean square voltage) of IC.

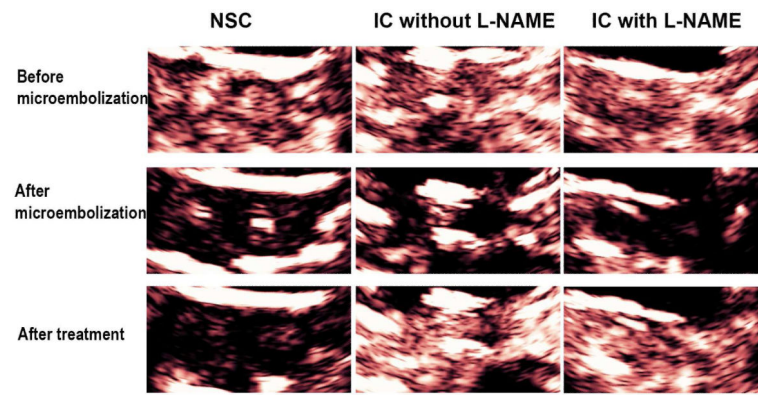


Figure 2. Examples of improvement in microvascular blood volume in a rat treated with intermittent IC inducing pulses both in the presence and absence of L-NAME pre-treatment
A rat treated with non-destructive stable cavitation imaging alone (NSC) is shown along the left column.

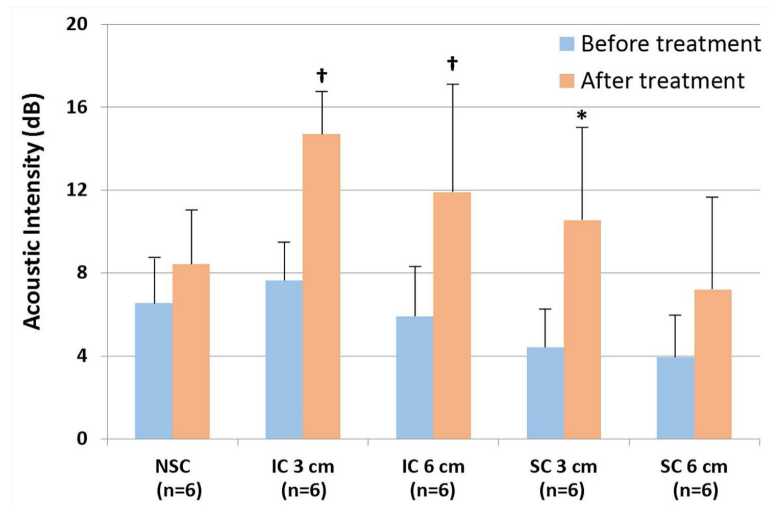


Figure 3. Demonstration of the increase in skeletal MBV with inertial cavitation (IC) inducing ultrasound treatments

Error bars depict standard deviation. SC = stable cavitation; NSC = nondestructive stable cavitation; 3 cm = 3 cm phantom; 6 cm = 6 cm phantom. * <0.05 compared to before treatment; † <0.01 compared to before treatment. n = 6 for each group.

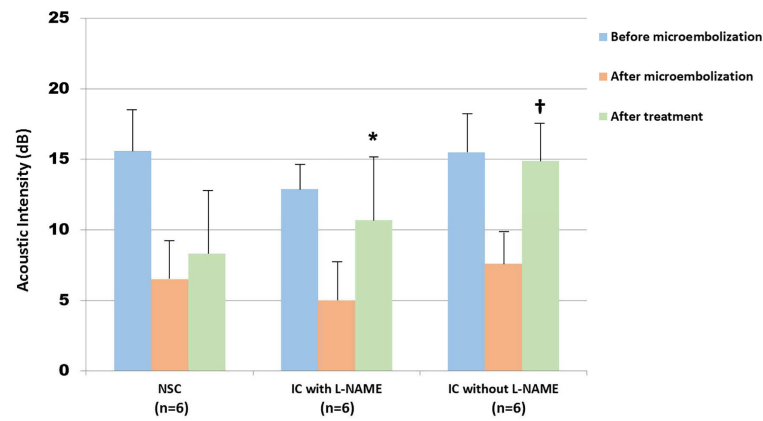


Figure 4. Effect of pretreatment with L-NAME on restoration of microvascular blood volume
Skeletal muscle intensity bar graphs after microembolization. The skeletal muscle intensity following IC inducing impulses (green bar graphs) increased to nearly the same level as in the absence of L-NAME pretreatment (blue histograms). * <0.01 compared to before treatment; † <0.001 compared to before treatment. $n = 6$ for each group.

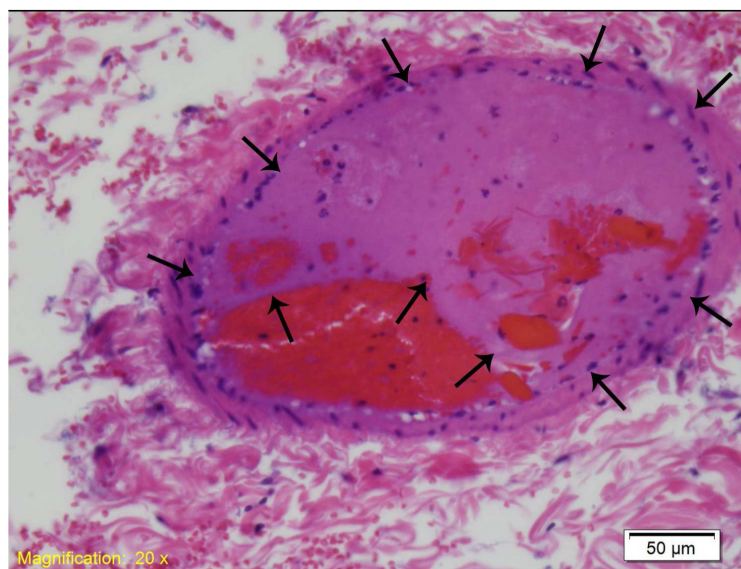


Figure 5.
An example of a residual thrombus (arrows) in a small vessel, seen in an L-NAME pre treated rat.

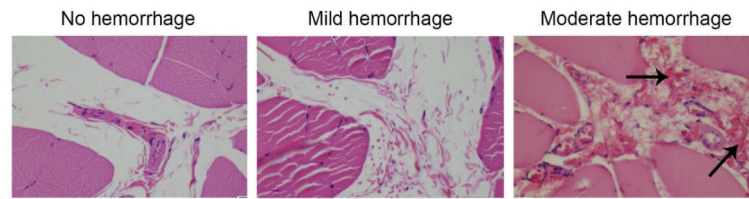


Figure 6. Examples of no, mild, and moderate peri-vascular hemorrhage

The arrows depict the red blood cells observed in extravascular foci. When two or more foci were observed in a 10x magnification plane, it was considered moderate hemorrhage.

Table 1

Peak negative pressures, image depths, focal depths, and therapeutic high mechanical index frame rates for inertial cavitation and stable cavitation inducing impulses from the diagnostic transducer. The measured peak negative pressures in water for the transducer were 1319 kPa at the IC setting and 600 kPa at the SC setting.

	3 cm TMP		6 cm TMP	
	IC	SC	IC	SC
Image depth	6 cm	6 cm	9 cm	9 cm
Focal depth	5 cm	5 cm	8 cm	8 cm
High MI frame rate	10 Hz	10 Hz	10 Hz	10 Hz
Attenuation (db)	2.352	4.704	2.352	4.704
Attenuation ratio	1.31	1.72	1.31	1.72
PNP after TMP [*]	1006	767	458	349

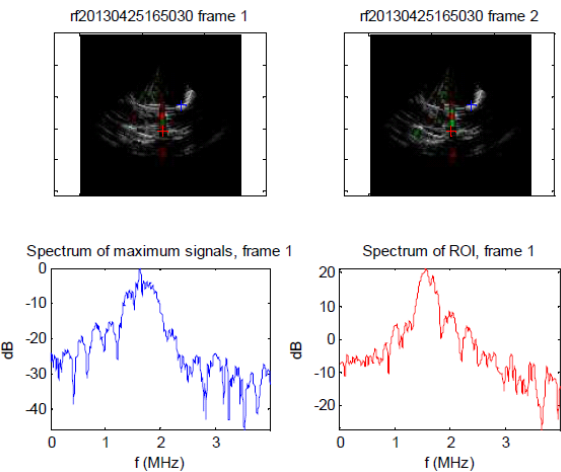
IC=inertial cavitation, SC=stable cavitation, MI=mechanical index; PNP=peak negative pressure; TMP=tissue mimicking phantom;

^{*} Hydrophone measurements were adjusted by known attenuation values for the TMP.

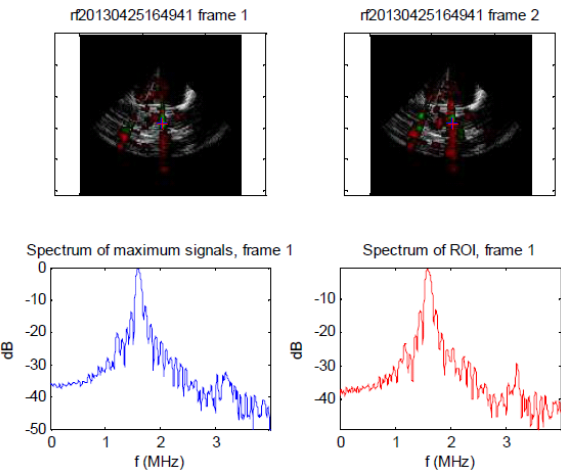
Table 2

Root mean square (RMS) values for inertial cavitation activity recorded from the microvasculature by the passive cavitation detectors at the different therapeutic impulse settings. At the MI 1.6 setting, there was a significant increase in the magnitude of IC activity recorded by the PCDs which corresponded to the increased noise noted on the accompanying radiofrequency spectrum (lower display). At 0.8 MI (middle panel), there was a significantly less RMS voltage, and the returning radiofrequency display indicates sub and ultraharmonic indicative of dominant SC (middle image). The N values represent the number of times the particular setting was tested in the total of four rats examined. N=number of times the particular MI setting was tested

Pulse Duration	MI 1.6 RMS (n=13)	MI 0.8 RMS (n=14)	MI 0.3 RMS (n=14)
20 us	4.051 ± 0.900 V	1.028 ± 0.315 V	0.083 ± 0.035 V



MI 0.8-Dominant SC inducing impulses (as indicated by the sub and ultra harmonic spikes on radiofrequency spectrum from two different regions of interest (red and blue) within the skeletal muscle preparation during a 10% Definity infusion.



MI 1.6 –Dominant IC radiofrequency spectrum observed from the same two regions of interest as indicated by absence of sub and ultraharmonic peaks and increased noise floor. Note the highest RMS value was for this setting, consistent with greater IC activity.

Author Manuscript

Author Manuscript

Author Manuscript

Author Manuscript

Table 3

Post mortem hemotoxylin and eosin staining examining for >50% residual thrombus in the small and medium-sized arterioles within the skeletal muscle preparations as well as for degrees of perivascular and interstitial hemorrhage. The denominators represent number of total sections (up to three per rat; 6 rats in each group) in which an observation was noted. For perivascular hemorrhage assessments, all sections were summed for a final grade.

Group	IC 3 cm TMP	IC 6 cm TMP	SC 3 cm TMP	SC 6 cm TMP	NSC (Low MI only)	IC 3 cm TMP/L NAME
>50% residual arteriolar thrombus	12/17	12/18	9/16	10/17	9/17	4/17 [*]
Significant perivascular hemorrhage	1/6	1/6	1/6	0/6	1/6	4/6 [†]

* p<0.05 compared to IC 3cm TMP, IC 6 cm TMP, and SC 6 cm TMP.

† p<0.05 compared to SC 6 cm.